N73-12933

NASA TECHNICAL NOTE

NASA TN D-7119

NASA TN D-7119

ELASTOSTATIC STRESS ANALYSIS OF ORTHOTROPIC RECTANGULAR CENTER-CRACKED PLATES

by George S. Gyekenyesi and Alexander Mendelson

Lewis Research Center

Cleveland, Ohio 44135

NATIONAL AERONAUTICS AND SPACE ADMINISTRATION • WASHINGTON, D. C. • NOVEMBER 1972

1. Report No.
NASA TN D-7119

2. Government Accession No.

3. Recipient's Catalog No.

4. Title and Subtitle
ELASTOSTATIC STRESS ANALYSIS OF ORTHOTROPIC RECTANGULAR CENTER-CRACKED PLATES

5. Report Date
November 1972

6. Performing Organization Code

7. Author(s)
George S. Gyekenyesi and Alexander Mendelson

8. Performing Organization Report No.
E-6889

9. Performing Organization Name and Address
Lewis Research Center
National Aeronautics and Space Administration
Cleveland, Ohio 44135

10. Work Unit No.
501-22

11. Contract or Grant No.

12. Sponsoring Agency Name and Address
National Aeronautics and Space Administration
Washington, D.C. 20546

13. Type of Report and Period Covered
Technical Note

14. Sponsoring Agency Code

15. Supplementary Notes

16. Abstract
A mapping-collocation method was developed for the elastostatic stress analysis of finite, anisotropic plates with centrally located traction-free cracks. The method essentially consists of mapping the crack into the unit circle and satisfying the crack boundary conditions exactly with the help of Muskhelishvili's function extension concept. The conditions on the outer boundary are satisfied approximately by applying the method of least-squares boundary collocation. A parametric study of finite-plate stress intensity factors, employing this mapping-collocation method, is presented. It shows the effects of varying material properties, orientation angle, and crack-length-to-plate-width and plate-height-to-plate-width ratios for rectangular orthotropic plates under constant tensile and shear loads.

17. Key Words (Suggested by Author(s))
Fracture mechanics
Elasticity
Anisotropy
Cracks
Plates

18. Distribution Statement
Unclassified - unlimited

19. Security Classif. (of this report)
Unclassified

20. Security Classif. (of this page)
Unclassified

21. No. of Pages
32

22. Price*
$3.00

* For sale by the National Technical Information Service, Springfield, Virginia 22151

ELASTOSTATIC STRESS ANALYSIS OF ORTHOTROPIC RECTANGULAR CENTER-CRACKED PLATES

by George S. Gyekenyesi and Alexander Mendelson

Lewis Research Center

SUMMARY

A mapping-collocation method was developed for the elastostatic stress analysis of finite, anisotropic plates with centrally located traction-free cracks. The method essentially consists of mapping the crack into the unit circle and satisfying the crack boundary conditions exactly with the help of Muskhelishvili's function extension concept. The conditions on the outer boundary are satisfied approximately by applying the method of least-squares boundary collocation.

A parametric study of finite-plate stress intensity factors, employing this mapping-collocation method, is presented. It shows the effects of varying material properties, orientation angle, and crack-length-to-plate-width and plate-height-to-plate-width ratios for rectangular orthotropic plates under constant tensile and shear loads.

INTRODUCTION

Anisotropic materials are frequently applied in present-day structural design, as exemplified in composite materials. Therefore, the problems pertaining to the stress distribution in finite and quasi-infinite plates of such materials containing cracks are of immediate importance. The infinite-plate problems present no difficulty (refs. 1 to 8); however, the problems of finite anisotropic plates with cracks remained fairly neglected until quite recently (refs. 9 to 11).

The mapping-collocation method as applied in this report was developed in reference 10 and parallels Bowie's mapping-collocation technique (ref. 12) for a finite isotropic plate with a central traction-free crack.

This report analyzes the effects of varying material properties, orientation angle, and crack-length-to-plate-width and plate-height-to-plate-width ratios on both the opening- and sliding-mode stress intensity factors in a rectangular orthotropic plate

with a centrally located traction-free crack under constant tensile and shear loads.

In addition to the parametric investigation, a brief summary of the development of the mapping-collocation method is presented; however, for a detailed exposition the reader is referred to reference 10.

SYMBOLS

The following list contains the more commonly used symbols and their representative meaning unless otherwise defined in the text. In general, all symbols are defined when first introduced.

A_{1n}	n^{th} complex constant in Laurent series associated with positive exponent terms
a	half-crack length
B_{1n}	n^{th} complex constant in Laurent series associated with negative exponent terms
C_{ij}	ij^{th} element of elastic compliance matrix
$\mathscr{C}_{1n}$	n^{th} modified complex constant associated with positive exponent terms in Laurent series
$\mathscr{C}_{2n}$	n^{th} modified complex constant associated with negative exponent terms in Laurent series
$\mathscr{C}_c$	complex constant depending on material properties
$\mathscr{C}_s, \mathscr{C}_d$	modified complex constants depending on sum and difference of A_{11} and B_{11}, respectively
c	half-width of rectangular plate
E_{11}, E_{22}	Young's moduli of elasticity with respect to coordinate directions
$F_{1n}, F_{2n}, G_{1n}, G_{2n}$	complex quantities utilized in construction of coefficient matrix in least-squares boundary collocation method
G_{12}	shear modulus of an orthotropic material
H_1, H_2	nondimensional opening- and sliding-mode stress intensity factors, respectively
h	half-height of a rectangular plate
K_1, K_2	opening- and sliding-mode stress intensity factors, respectively

M	total number of collocation points on outer boundary of region with central crack
NN, NP	truncation numbers on infinite sums associated with negative and positive exponent terms in Laurent series, respectively
T_s	constant shear stress applied to boundary of square plate
T_t	constant tensile stress applied to boundary of rectangular plate
x, y	rectangular coordinates
z	conventional complex variable
z_1, z_2	complex variables modified by material properties
δ	material orientation angle
ζ, ζ_k	complex variables in parametric planes
ν_{12}	Poisson's ratio in an orthotropic material
μ_1, μ_2	Lekhnitskii's material parameters
$\sigma_{xx}, \sigma_{yy}, \sigma_{xy}$	components of stress tensor, rectangular coordinates
φ	Airy's stress function
$\varphi_1(z_1), \varphi_2(z_2)$	complex stress potential functions

BRIEF DESCRIPTION OF MAPPING-COLLOCATION METHOD

Consider a doubly connected orthotropic region L defined by a crack Γ_c and the region's outer boundary Γ, as shown in figure 1(a). The crack and its exterior can be mapped, as shown, into the unit circle γ and its exterior L_ζ by the mapping function

$$\zeta = \frac{z + \sqrt{z^2 - a^2}}{a} \tag{1}$$

where z is the usual complex variable, x + iy.

We introduce two additional complex variables, z_1 and z_2, defined by

$$z_k = \frac{1 - i\mu_k}{2} z + \frac{1 + i\mu_k}{2} \bar{z} \qquad k = 1, 2 \tag{2}$$

where μ_k and $\bar{\mu}_k$ are the roots of the characteristic equation

$$C_{22} - 2C_{26}\mu + (C_{66} + 2C_{12})\mu^2 - 2C_{16}\mu^3 + C_{11}\mu^4 = 0 \tag{3}$$

and the C_{ij} are the material compliances appearing in the generalized Hooke's law for an orthotropic material.

The regions L_k with the boundaries Γ_{ck} and Γ_k obtained by the transformation (2) can also be mapped into their respective ζ_k-planes by the mapping functions

$$\zeta_k = \frac{z_k + \sqrt{z_k^2 - a^2}}{a} \qquad k = 1, 2 \tag{4}$$

as illustrated in figures 1(b) and (c).

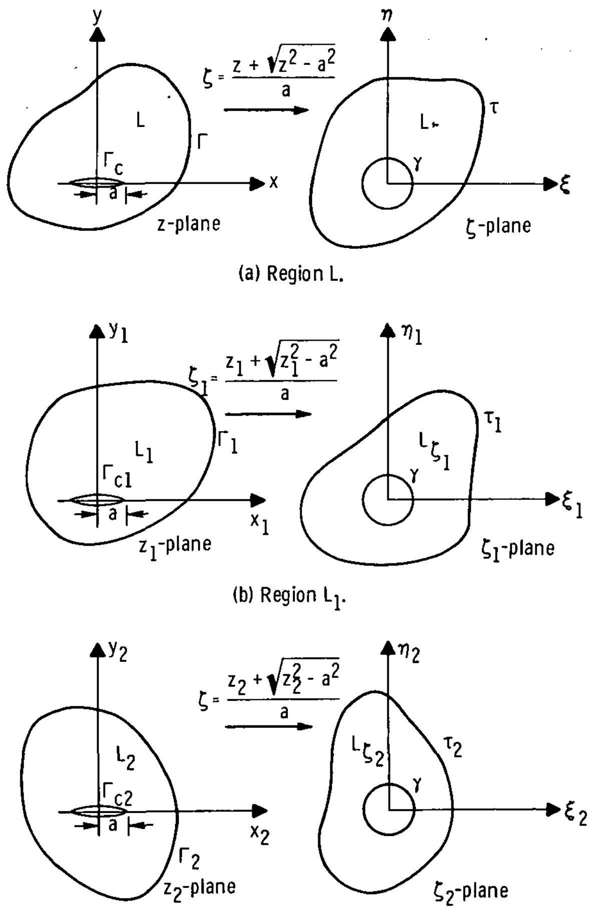

Figure 1. - Mapping of doubly connected regions L, L_1, and L_2 into their corresponding parametric planes.

The Airy stress function $\varphi(x, y)$ can be written in terms of two analytic functions of the complex variables z_1 and z_2:

$$\varphi(x, y) = \mathcal{R}e\left[F_1(z_1) + F_2(z_2)\right] \tag{5}$$

With the following definitions:

$$\varphi_1(z_1) = \frac{dF_1}{dz_1}$$

and

$$\varphi_2(z_2) = \frac{dF_2}{dz_2}$$

the zero traction conditions on the crack can be satisfied by applying Muskhelishvili's function extension concept across the unit circle (ref. 13). This is accomplished by expressing one of the unknown complex stress potentials in terms of the other. If $\varphi_2(\zeta_2)$ is chosen as

$$\varphi_2(\zeta_2) = \frac{\bar{\mu}_2 - \bar{\mu}_1}{\mu_2 - \bar{\mu}_2}\,\bar{\varphi}_1\left(\frac{1}{\zeta_2}\right) + \frac{\bar{\mu}_2 - \mu_1}{\mu_2 - \bar{\mu}_2}\,\varphi_1(\zeta_2) \tag{6}$$

the crack boundary conditions will be satisfied for any choice of $\varphi_1(\zeta_1)$, provided it is analytic.

The substitution of expression (6) into the boundary conditions for the outer boundary of the region results in two conditions given completely in terms of $\varphi_1(\zeta_1)$, $\varphi_1(\zeta_2)$, and $\bar{\varphi}_1(1/\zeta_2)$.

The determination of $\varphi_1(\zeta_1)$ depends on its form of representation and the satisfaction of the boundary conditions on the outer boundary. Specifically, it is assumed that $\varphi_1(\zeta_1)$ can be represented in the form of a truncated Laurent series, such that

$$\varphi_1(\zeta_1) = A_{10} + \sum_{n=1}^{NP} A_{1n}\zeta_1^n + \sum_{n=1}^{NN} B_{1n}\zeta_1^{-n} \tag{7}$$

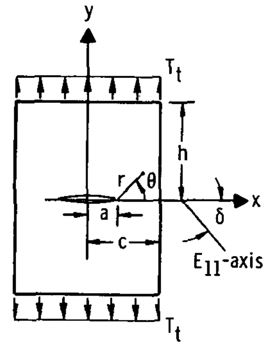

Figure 2. - Tension problem of rectangular plate with central crack.

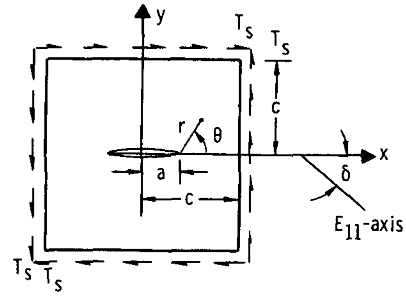

Figure 3. - Shear problem of square plate with central crack.

Because of the symmetry conditions for the orthotropic plate problems in question (figs. 2 and 3), n becomes necessarily odd and the final forms of the boundary conditions for the outer boundary are obtained as

$$
\begin{bmatrix}
0 & \mathscr{R}e\,F_{11} & -\mathscr{I}m\,F_{11} & \cdots & \mathscr{R}e\,F_{1NP} & -\mathscr{I}m\,F_{1NP} & \cdots & \mathscr{R}e\,F_{2NN} & -\mathscr{I}m\,F_{2NN} \\
y & \mathscr{R}e\,G_{11} & -\mathscr{I}m\,G_{11} & \cdots & \mathscr{R}e\,G_{1NP} & -\mathscr{I}m\,G_{1NP} & \cdots & \mathscr{R}e\,G_{2NN} & -\mathscr{I}m\,G_{2NN}
\end{bmatrix}
\begin{bmatrix}
\mathscr{R}e\left[\mathscr{C}_c\ \mathscr{C}_s\right] \\
\mathscr{R}e\,\mathscr{C}_D \\
\mathscr{I}m\,\mathscr{C}_D \\
\vdots \\
\mathscr{R}e\,\mathscr{C}_{1NP} \\
\mathscr{I}m\,\mathscr{C}_{1NP} \\
\vdots \\
\mathscr{R}e\,\mathscr{C}_{2NN} \\
\mathscr{I}m\,\mathscr{C}_{2NN}
\end{bmatrix}
= \frac{1}{2}\begin{bmatrix} T_t x - T_s y \\ -T_s x \end{bmatrix} \qquad z \text{ in } \Gamma \qquad (8)
$$

where NN and NP are odd. The terms in equations (8) are defined as

$$
\left.
\begin{aligned}
\mathscr{C}_s &= \frac{A_{11} + B_{11}}{a(\mu_2 - \bar{\mu}_2)} \\
\mathscr{C}_d &= \frac{A_{11} - B_{11}}{a(\mu_2 - \bar{\mu}_2)} \\
\mathscr{C}_{1n} &= \frac{A_{1n}}{a^n(\mu_2 - \bar{\mu}_2)} \\
\mathscr{C}_{2n} &= \frac{B_{1n}}{a^n(\mu_2 - \bar{\mu}_2)} \\
\mathscr{C}_c &= (\mu_2 - \mu_1)(\mu_2 - \bar{\mu}_2)(\bar{\mu}_2 - \mu_1) \\
F_{11} &= (\mu_2 - \bar{\mu}_2)\sqrt{z_1^2 - a^2} + (\bar{\mu}_2 - \mu_1)\sqrt{z_2^2 - a^2} + (\mu_2 - \mu_1)\sqrt{\bar{z}_2^2 - a^2} \\
G_{11} &= \mu_1(\mu_2 - \bar{\mu}_2)\sqrt{z_1^2 - a^2} + \mu_2(\bar{\mu}_2 - \mu_1)\sqrt{z_2^2 - a^2} + \bar{\mu}_2(\mu_2 - \mu_1)\sqrt{\bar{z}_2^2 - a^2} \\
F_{1n} &= (\mu_2 - \bar{\mu}_2)\left(z_1 + \sqrt{z_1^2 - a^2}\right)^n + (\bar{\mu}_2 - \mu_1)\left(z_2 + \sqrt{z_2^2 - a^2}\right)^n + (\mu_1 - \mu_2)\left(\bar{z}_2 - \sqrt{\bar{z}_2^2 - a^2}\right)^n \\
F_{2n} &= (\mu_2 - \bar{\mu}_2)\left(z_1 - \sqrt{z_1^2 - a^2}\right)^n + (\bar{\mu}_2 - \mu_1)\left(z_2 - \sqrt{z_2^2 - a^2}\right)^n + (\mu_1 - \mu_2)\left(\bar{z}_2 + \sqrt{\bar{z}_2^2 - a^2}\right)^n \\
G_{1n} &= \mu_1(\mu_2 - \bar{\mu}_2)\left(z_1 + \sqrt{z_1^2 - a^2}\right)^n + \mu_2(\bar{\mu}_2 - \mu_1)\left(z_2 + \sqrt{z_2^2 - a^2}\right)^n + \bar{\mu}_2(\mu_1 - \mu_2)\left(\bar{z}_2 - \sqrt{\bar{z}_2^2 - a^2}\right)^n \\
G_{2n} &= \mu_1(\mu_2 - \bar{\mu}_2)\left(z_1 - \sqrt{z_1^2 - a^2}\right)^n + \mu_2(\bar{\mu}_2 - \mu_1)\left(z_2 - \sqrt{z_2^2 - a^2}\right)^n + \bar{\mu}_2(\mu_1 - \mu_2)\left(\bar{z}_2 + \sqrt{\bar{z}_2^2 - a^2}\right)^n
\end{aligned}
\right\} \quad (9)
$$

Equations (8) must now be solved for the unknowns, $\mathscr{C}_{1n}$ and $\mathscr{C}_{2n}$. The applicability of the least-squares boundary collocation method (refs. 14 and 15) to the problems at hand is readily obvious. Equations (8) are to be approximately satisfied at M points on the outer boundary, while the number of unknowns is given by NN + NP + 1. Then the resulting matrix equation can be written as

$$\underset{2M\times(NN+NP+1)}{\mathscr{E}}\;\underset{(NN+NP+1)\times 1}{\mathscr{C}} = \underset{2M\times 1}{\mathscr{X}} \tag{10}$$

For the least-squares boundary collocation method, the problem becomes

$$\mathscr{E}^T\mathscr{E}\mathscr{C}^* = \mathscr{E}^T\mathscr{X} \tag{11}$$

where $\mathscr{C}^*$ is the desired solution vector.

The solution of equation (11) was carried out on a digital computer by declaring all quantities and operations in double precision and utilizing the Gauss-elimination technique with complete pivoting. It should also be mentioned that the elements of the coefficient matrix $\mathscr{E}$ were scaled by the devisor

$$R^n = \left(\sqrt{c^2 + h^2}\right)^n$$

After the approximate solution vector $\mathscr{C}^*$ is obtained, the computation of the stress intensity factors and the stress components is a matter of substitution of the elements of $\mathscr{C}^*$ into the following expressions:

$$K_1 = \frac{4}{\sqrt{a}} \mathcal{R}e\left[(\mu_2 - \mu_1)\left(a\mathscr{C}_D + \sum_{n=3,5,7}^{NP} na^n\mathscr{C}_{1n} - \sum_{n=3}^{NN} na^n\mathscr{C}_{2n}\right)\right] \tag{12}$$

$$K_2 = -\frac{4}{\sqrt{a}} \mathcal{R}e\left[\overline{\mu}_2(\mu_2 - \mu_1)\left(a\mathscr{C}_D + \sum_{n=3,5,7}^{NP} na^n\mathscr{C}_{1n} - \sum_{n=3}^{NN} na^n\mathscr{C}_{2n}\right)\right] \tag{13}$$

$$
\begin{aligned}
\sigma_{xx} = {} & 2\mathcal{R}e\left[\mathscr{C}_c \mathscr{C}_s\right] + 2\mathcal{R}e\left\{\mathscr{C}_d\left[\mu_1^2(\mu_2 - \overline{\mu}_2)\frac{z_1}{\sqrt{z_1^2 - a^2}} + \mu_2^2(\overline{\mu}_2 - \mu_1)\frac{z_2}{\sqrt{z_2^2 - a^2}} + \overline{\mu}_2^2(\mu_2 - \mu_1)\frac{z_2}{\sqrt{\overline{z}_2^2 - a^2}}\right]\right\} \\
& + 2\mathcal{R}e\sum_{n=3,5,7}^{NP}\left\{n\mathscr{C}_{1n}\left[\frac{\mu_1^2(\mu_2 - \overline{\mu}_2)}{\sqrt{z_1^2 - a^2}}\left(z_1 + \sqrt{z_1^2 - a^2}\right)^n + \frac{\mu_2^2(\overline{\mu}_2 - \mu_1)}{\sqrt{z_2^2 - a^2}}\left(z_2 + \sqrt{z_2^2 - a^2}\right)^n + \frac{\overline{\mu}_2^2(\mu_2 - \mu_1)}{\sqrt{\overline{z}_2^2 - a^2}}\left(\overline{z}_2 - \sqrt{\overline{z}_2^2 - a^2}\right)^n\right]\right\} \\
& - 2\mathcal{R}e\sum_{n=3,5,7}^{NN}\left\{n\mathscr{C}_{2n}\left[\frac{\mu_1^2(\mu_2 - \overline{\mu}_2)}{\sqrt{z_1^2 - a^2}}\left(z_1 - \sqrt{z_1^2 - a^2}\right)^n + \frac{\mu_2^2(\overline{\mu}_2 - \mu_1)}{\sqrt{z_2^2 - a^2}}\left(z_2 - \sqrt{z_2^2 - a^2}\right)^n + \frac{\overline{\mu}_2(\mu_2 - \mu_1)}{\sqrt{\overline{z}_2^2 - a^2}}\left(\overline{z}_2 + \sqrt{\overline{z}_2^2 - a^2}\right)^n\right]\right\}
\end{aligned}
\tag{14}
$$

$$
\begin{aligned}
\sigma_{yy} = {} & 2\mathcal{R}e\left\{\mathscr{C}_d\left[(\mu_2 - \overline{\mu}_2)\frac{z_1}{\sqrt{z_1^2 - a^2}} + (\overline{\mu}_2 - \mu_1)\frac{z_2}{\sqrt{z_2^2 - a^2}} + (\mu_2 - \mu_1)\frac{\overline{z}_2}{\sqrt{\overline{z}_2^2 - a^2}}\right]\right\} \\
& + 2\mathcal{R}e\sum_{n=3,5,7}^{NP}\left\{n\mathscr{C}_{1n}\left[\frac{\mu_2 - \overline{\mu}_2}{\sqrt{z_1^2 - a^2}}\left(z_1 + \sqrt{z_1^2 - a^2}\right)^n + \frac{\overline{\mu}_2 - \mu_1}{\sqrt{z_2^2 - a^2}}\left(z_2 + \sqrt{z_2^2 - a^2}\right)^n + \frac{\mu_2 - \mu_1}{\sqrt{\overline{z}_2^2 - a^2}}\left(\overline{z}_2 - \sqrt{\overline{z}_2^2 - a^2}\right)^n\right]\right\} \\
& - 2\mathcal{R}e\sum_{n=3,5,7}^{NN}\left\{n\mathscr{C}_{2n}\left[\frac{\mu_2 - \overline{\mu}_2}{\sqrt{z_1^2 - a^2}}\left(z_1 - \sqrt{z_1^2 - a^2}\right)^n + \frac{\overline{\mu}_2 - \mu_1}{\sqrt{z_2^2 - a^2}}\left(z_2 - \sqrt{z_2^2 - a^2}\right)^n + \frac{\mu_2 - \mu_1}{\sqrt{\overline{z}_2^2 - a^2}}\left(\overline{z}_2 + \sqrt{\overline{z}_2^2 - a^2}\right)^n\right]\right\}
\end{aligned}
\tag{15}
$$

$$- 2\,\mathcal{R}e \sum_{n=3,5,7}^{NP} \left\{ n\mathscr{C}_{1n} \left[\frac{\mu_1(\mu_2 - \bar{\mu}_2)}{\sqrt{z_1^2 - a^2}} \left(z_1 + \sqrt{z_1^2 - a^2} \right)^n + \frac{\mu_2(\bar{\mu}_2 - \mu_1)}{\sqrt{z_2^2 - a^2}} \left(z_2 + \sqrt{z_2^2 - a^2} \right)^n + \frac{\bar{\mu}_2(\mu_2 - \mu_1)}{\sqrt{\bar{z}_2^2 - a^2}} \left(\bar{z}_2 - \sqrt{\bar{z}_2^2 - a^2} \right)^n \right] \right\}$$

$$+ 2\,\mathcal{R}e \sum_{n=3,5,7}^{NN} \left\{ n\mathscr{C}_{2n} \left[\frac{\mu_1(\mu_2 - \bar{\mu}_2)}{\sqrt{z_1^2 - a^2}} \left(z_1 - \sqrt{z_1^2 - a^2} \right)^n + \frac{\mu_2(\bar{\mu}_2 - \mu_1)}{\sqrt{z_2^2 - a^2}} \left(z_2 - \sqrt{z_2^2 - a^2} \right)^n + \frac{\bar{\mu}_2(\mu_2 - \mu_1)}{\sqrt{\bar{z}_2^2 - a^2}} \left(\bar{z}_2 + \sqrt{\bar{z}_2^2 - a^2} \right)^n \right] \right\} \tag{16}$$

For a detailed discussion and complete derivation of the above method, refer to reference 10.

RESULTS AND DISCUSSION OF SOLUTIONS OF TENSION AND SHEAR PROBLEMS

Specifications of Parameters

The solutions of the two problems shown in figures 2 and 3 are based on the following specifications:

(1) The nondimensional stress intensity factors H_K are defined as $H_k = K_k/\sqrt{a}\,T_t$ for tension and $H_k = K_k/\sqrt{a}\,T_s$ for shear (k = 1, 2).

(2) With the exception of the investigation of the effects of material properties on the stress intensity factors, the ratios

$$\frac{E_{22}}{E_{11}} = 0.366$$

and

$$\frac{\frac{E_{11}}{E_{22}}}{\left(\frac{E_{11}}{2G_{12}} - \nu_{12}\right)^2} = 0.257$$

were used throughout the entire analysis. These ratios correspond to the properties of fiberglass.

(3) In studying the effects of varying material properties on the stress intensity factors in both the tension and shear problems, the following parameter ranges were considered:

$$0.05 \le \frac{E_{22}}{E_{11}} \le 1$$

$$0.001 \le \frac{\frac{E_{11}}{E_{22}}}{\left(\frac{E_{11}}{2G_{12}} - \nu_{12}\right)^2} \le \infty$$

$$\frac{a}{c} = \frac{2}{3} \qquad \frac{h}{c} = 1 \qquad \delta = 45^{\circ}$$

(4) In studying the effects of varying plate aspect ratio h/c and crack-length-to-plate-width ratio a/c on the stress intensity factors in the tension problem, the parameter ranges were chosen as follows:

$$0 < \frac{a}{c} \le \frac{2}{3}$$

$$0.25 \le \frac{h}{c} \le 133$$

$$\delta = 45^{\circ}$$

(5) The effects of variation of the orientation angle δ were also analyzed for both the tension and shear problems, considering the following parameter ranges:

$$0 < \frac{a}{c} \leq \frac{2}{3}$$

$$0^{o} \leq \delta \leq 90^{o}$$

$$\frac{h}{c} = 1$$

Examination of Mapping-Collocation Method

The available results which can be used to check the accuracy of this method are those for centrally cracked infinite plates (refs. 1 and 3) and the results of Kobayashi, Isida, and Sawyer (refs. 16 to 18) for finite isotropic rectangular plates. In order to gain a certain degree of confidence in the mapping-collocation method, both the results for the infinite orthotropic and finite isotropic plates were verified.

The first verification is obtained by making the plate dimensions large compared to the crack length.

This resulted in $H_1 = 1.0000$ and $H_2 = 0.0000$. The corresponding analytical results for an infinite plate are $H_1 = 1$ and $H_2 = 0$. It was, however, also noted that the satisfaction of the stress boundary conditions markedly improved with the use of more and more terms in the Laurent series expansion of $\varphi_1(\zeta_1)$. Thus, the results of the infinite plates were verified for both the tension and shear problems.

The verification of Kobayashi's, Isida's, and Sawyer's opening-mode stress intensity factors for various finite isotropic rectangular plates in tension was carried out by setting the ratios

$$\frac{E_{22}}{E_{11}} = 1$$

and

$$\frac{\frac{E_{11}}{E_{22}}}{\left(\frac{E_{11}}{2G_{12}} - \nu_{12}\right)^2} = 1$$

The value of the orientation angle had no influence on the results. The cases considered are shown in table I, where the various stress intensity factors are tabulated and can readily be compared with each other. As can be seen from table I, agreement with the known results is excellent.

In order to economize the mapping-collocation method with regard to the use of the number of terms in the Laurent series expansion of $\varphi_1(\zeta_1)$, two different truncation numbers NN and NP were assigned as limits of the sums in the various expressions. The numbers NN and NP are odd for orthotropic materials and correspond to the number of the negative and positive exponent terms in the Laurent series expansion of the stress potential function $\varphi_1(\zeta_1)$. Upon investigating various NN/NP ratios for the finite plate problems, it was found that a NN/NP ratio of 5/3 resulted in fairly fast convergence with rather well-satisfied boundary conditions. This NN/NP ratio was retained throughout the whole investigation of the problems given in figures 2 and 3.

One of the most important indications of the degree of accuracy of the solutions obtained by the mapping-collocation method comes from the examination of the boundary stress between collocation points. Since the least-squares method of collocation results in the satisfaction of the boundary conditions only in the approximate sense, the magnitude and frequency of oscillations of the boundary stresses serve as an indicator to the "exactness" of the solution of the stress boundary-value problem. Thus, in each case, the boundary stresses were also examined. For example, in the case of a square plate in tension with $a/c = 2/3$ and $\delta = 45^{\circ}$, the largest error in the boundary stresses was found to be about 4 percent and it occurred in a sudden manner at the corners of the plate.

In addition, the pattern of convergence of the stress intensity factors H_1 and H_2 was also investigated. The results are shown in table II and figures 4 and 5. It was ob-

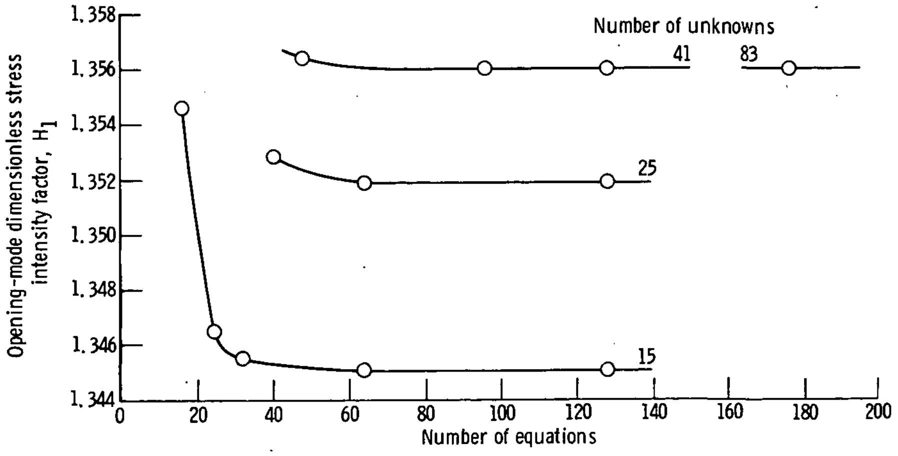

Figure 4. - Typical pattern of convergence of opening-mode stress intensity factor for tensile loading. Plate size, $h/c = 1$; crack length, $a/c = 1/2$; orientation angle, $\delta = 45^{0}$.

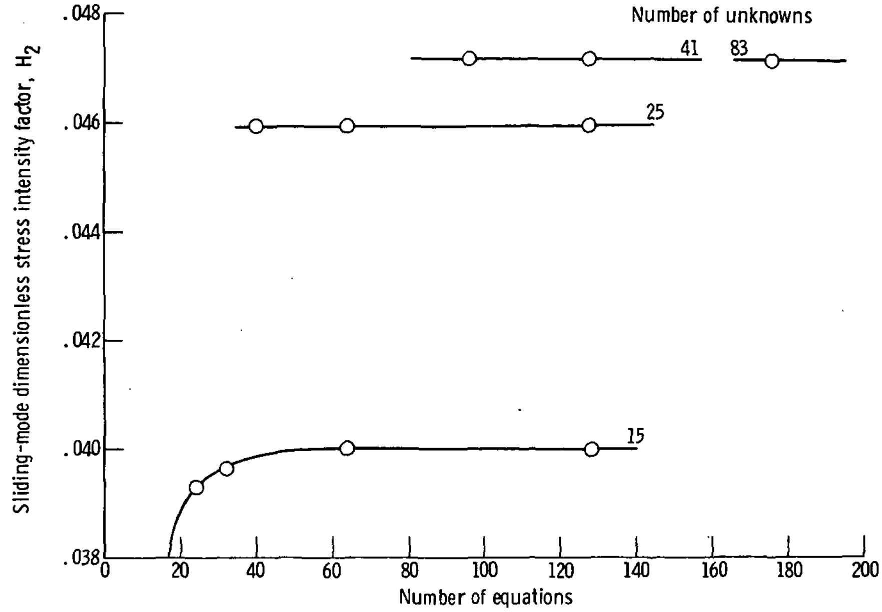

Figure 5. - Typical pattern of convergence of sliding-mode stress intensity factor for tensile loading. Plate size, h/c = 1; crack length, a/c = 1/2; orientation angle, $\delta = 45^{\circ}$.

served that the insensitiveness of H_1 and H_2 to a change in the number of terms of the Laurent series expansion of the stress potential $\varphi_1(\zeta_1)$ is an excellent indicator to how well the boundary conditions are satisfied by the least-squares approximation.

Upon considering various materials, plate sizes (aspect ratios), a/c ratios, and orientation angles under the loading conditions shown in figures 2 and 3, two conclusions became obvious regarding the convergence of the stress intensity factors:

(1) Convergence of the stress intensity factors is definitely affected by the material parameters. It was found, for example, that for a square plate in tension with $a/c = 2/3$ and $\delta = 45^{\circ}$, the use of the dimensionless material constant

$$\frac{\dfrac{E_{11}}{E_{22}}}{\left(\dfrac{E_{11}}{2G_{12}} - \nu_{12}\right)^2} = 0.0001$$

with any E_{22}/E_{11} ratio resulted in oscillatory values of H_1 and H_2. In this case, the number of unknowns was taken as 83, which gave excellent results for higher values of the dimensionless material constant.

(2) Convergence of the stress intensity factors is also affected by the a/c ratios. For a square plate in tension with

$$\frac{\dfrac{E_{11}}{E_{22}}}{\left(\dfrac{E_{11}}{2G_{12}} - \nu_{12}\right)^2} = 0.257$$

and with $E_{22}/E_{11} = 0.366$, $a/c = 0.9$, and $\delta = 45^{\circ}$ with the use of 83 unknowns, it was found that the boundary conditions were rather badly satisfied. The method probably resulted in unconverged stress intensity factors. For smaller a/c ratios, well-converged values of H_1 and H_2 were obtained.

SOLUTION OF TENSION PROBLEMS OF ORTHOTROPIC RECTANGULAR PLATE WITH CENTRAL CRACK

The consideration of the tension problem, that is, when the constant boundary stress is applied in the y-direction (fig. 2), resulted in various parametric studies involving material properties, a/c ratios, h/c ratios, and orientation angles.

Effects of Material Properties

An orthotropic material can be characterized by two dimensionless ratios constructed from the engineering material constants E_{11}, E_{22}, G_{12}, and ν_{12} (ref. 10). These dimensionless ratios are

$$\frac{E_{22}}{E_{11}} \quad \text{and} \quad \frac{\dfrac{E_{11}}{E_{22}}}{\left(\dfrac{E_{11}}{2G_{12}} - \nu_{12}\right)^2}$$

The effects of these two dimensionless ratios on the stress intensity factors are shown in table III and figures 6 and 7.

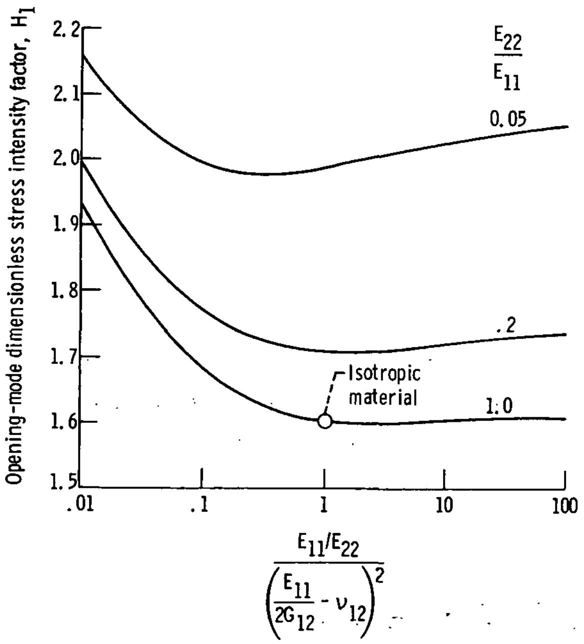

Figure 6. - Effects of material properties on opening-mode stress intensity factor for tensile loading. Plate size, h/c = 1; crack length, a/c = 2/3; orientation angle, $\delta = 45^{0}$.

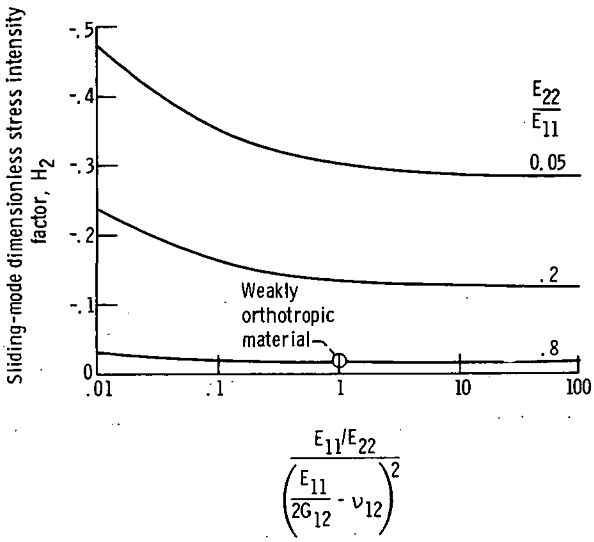

Figure 7. - Effects of material properties on sliding-mode stress intensity factor for tensile loading. Plate size, h/c = 1; crack length, a/c = 2/3; orientation angle, $\delta = 45^{0}$.

Figure 6 demonstrates the effects of the dimensionless material ratios on the opening-mode stress intensity factor, while figure 7 shows the sliding-mode stress intensity factor as a function of these two ratios. Figure 6 shows that, as the E_{22}/E_{11} ratio decreases, the opening-mode dimensionless stress intensity factor H_1 increases in value and that, for a fixed value of this ratio, the stress intensity factor exhibits a minimum value.

Figure 7 shows the interesting result that there exists a sliding-mode stress intensity factor for the case of a pure tensile load, contrary to the results for an infinite or isotropic plate. This results strictly from the orthotropy of the material and the finiteness of the plate dimensions. It may be noted that the maximum magnitude of the sliding-mode stress intensity factor shown in figure 7 is about 14 percent of the opening-mode stress intensity factor for the same E_{22}/E_{11} ratio.

Effects of Plate Dimensions

In order to investigate the effects of various plate widths and plate lengths on the stress intensity factors H_1 and H_2, the dimensionless material ratios were set at

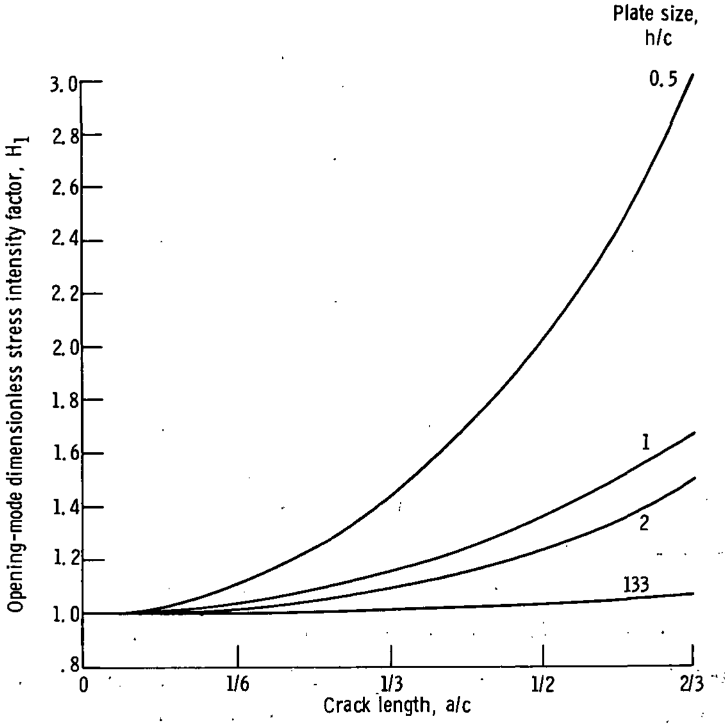

Figure 8. - Effects of plate width and plate size on opening-mode stress intensity factor for tensile loading. Orientation angle, $\delta = 45^0$.

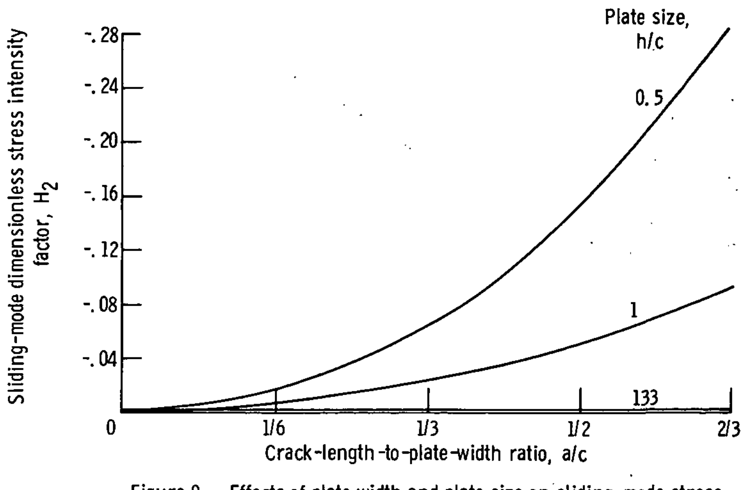

Figure 9. - Effects of plate width and plate size on sliding-mode stress intensity factor for tensile loading. Orientation angle, $\delta = 45^0$.

$$\frac{E_{22}}{E_{11}} = 0.366 \quad \text{and} \quad \frac{\dfrac{E_{11}}{E_{22}}}{\left(\dfrac{E_{11}}{2G_{12}} - \nu_{12}\right)^2} = 0.257$$

with an orientation angle $\delta = 45^{\circ}$. These ratios correspond approximately to fiberglass properties. The results are shown in table IV and figures 8 and 9.

Effects of Orientation Angle and Crack Length

For the investigation of the effects of the orientation angle and the crack length on the stress intensity factors, the h/c ratio was taken as 1 (square plate) and the dimensionless material ratios were held constant at the values specified previously.

The variations of the orientation angle δ and the a/c ratio resulted in table V. The graphs constructed from table V are presented in figures 10 and 11. Figure 10 shows the effects of various orientation angles δ on the opening-mode stress intensity factor H_1 for constant a/c ratios. Figure 11 shows the sliding-mode stress intensity

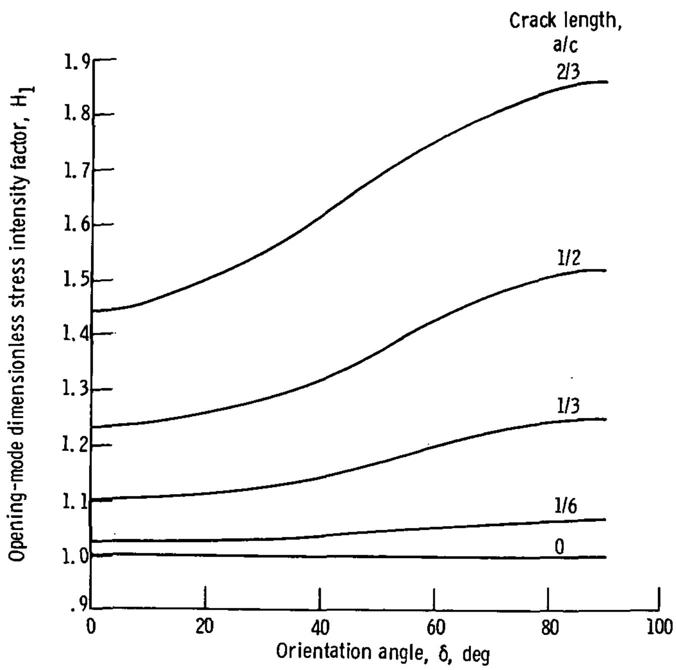

Figure 10. - Effects of orientation angle and plate width on opening-mode stress intensity factor for tensile loading. Plate size, h/c = 1.

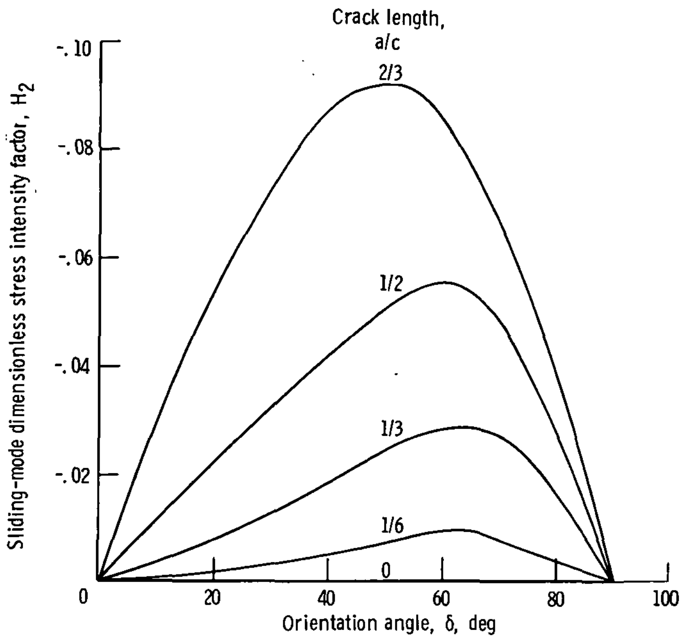

Figure 11. - Effects of orientation angle and plate width on sliding-mode stress intensity factor for tensile loading. Plate size, h/c = 1.

factor H_2 as affected by changes in δ and a/c.

As an illustration of the typical stress distribution on the line $y = 0$ for the range $1 < x/a \leq 3/2$, the values of the stress components were tabulated in table VI for a plate with $h/c = 1$, $a/c = 2/3$, $\delta = 45^{\circ}$ and plotted in figures 12 and 13.

The presence of σ_{xy} results from the general orthotropy of the material. It should also be observed that σ_{xy} becomes effectively zero on the boundary, which it should be for proper satisfaction of the boundary conditions.

For each H_1 and H_2 value obtained, the complete boundary-value problem of an orthotropic rectangular plate containing a central crack had to be solved. In each case, in addition to the computation of the stress components on the boundary, the stress components on the $y = 0$ line were also recorded. It gives one confidence in the method to know that for isotropic and specially orthotropic materials, the shear stress component σ_{xy} was effectively zero on the $y = 0$ line. Also for problems with $E_{22}/E_{11} = 1$, the shear stress component σ_{xy} on the $y = 0$ line was practically zero for any value of

$$\frac{\dfrac{E_{11}}{E_{22}}}{\left(\dfrac{E_{11}}{2G_{12}} - \nu_{12}\right)^2}$$

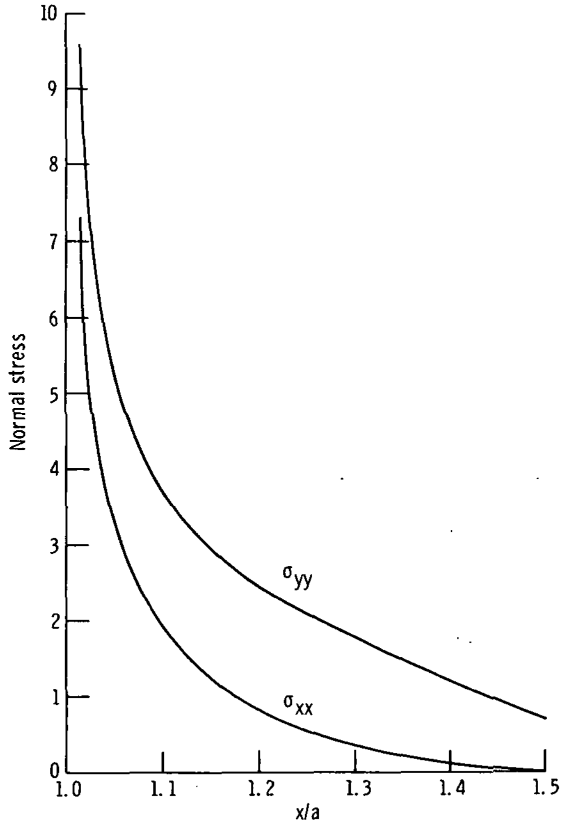

Figure 12. - Normal stress distribution on $y = 0$, $x > a$ line for tensile loading. Plate size, $h/c = 1$; crack length, $a/c = 2/3$; orientation angle, $\delta = 45^{\circ}$; constant tensile stress, $T_t = 1$.

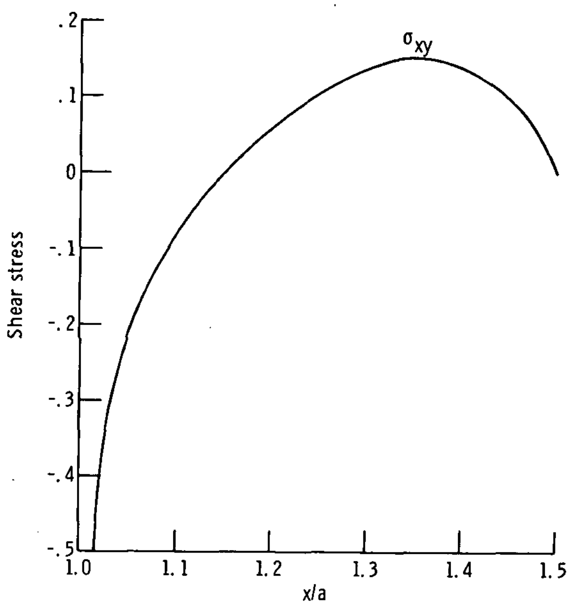

Figure 13. - Shear stress distribution on $y = 0$, $x > a$ line for tensile loading. Plate size, $h/c = 1$; crack length, $a/c = 2/3$; orientation angle, $\delta = 45^{\circ}$; constant tensile stress, $T_t = 1$.

SOLUTION OF SHEAR PROBLEM OF ORTHOTROPIC SQUARE PLATE WITH CENTRAL CRACK

In addition to the tension problem discussed in the preceding section, the problem of an orthotropic square plate containing a central crack and loaded by unit shear stress (fig. 3) was also considered. As in the case of the tension problem, the shear problem was also solved for various dimensionless material ratios, a/c ratios, and orientation angles. The h/c ratio was held constant ($h/c = 1$) throughout the entire analysis of the shear problem.

The results of the parametric study involving variations of the dimensionless material ratios while we held $a/c = 2/3$ and $\delta = 45^{\circ}$ are summarized in table VII and figures 14 and 15.

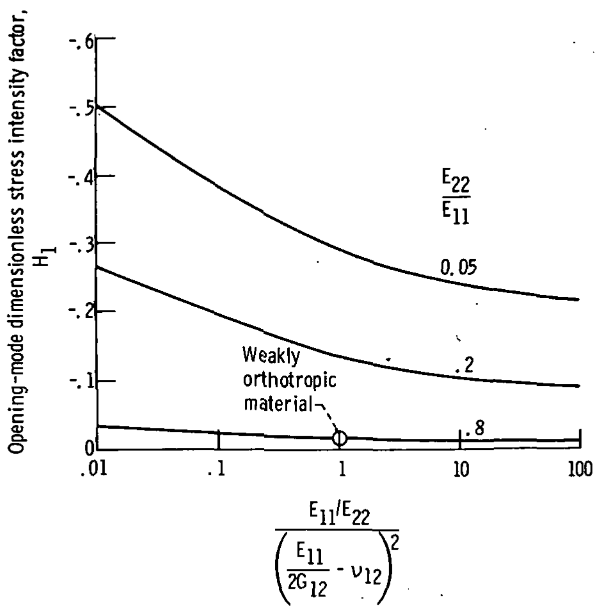

Figure 14. - Effects of material properties on opening-mode stress intensity factor for shear loading. Plate size, $h/c = 1$; crack length, $a/c = 2/3$; orientation angle, $\delta = 45^0$.

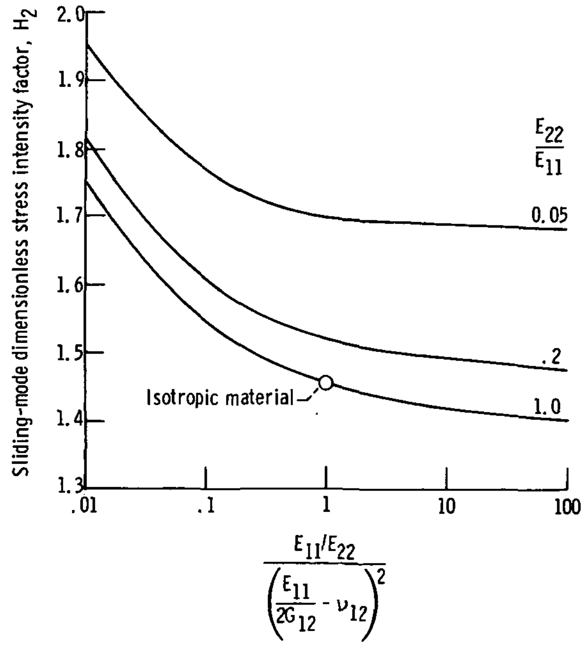

Figure 15. - Effects of material properties on sliding-mode stress intensity factor for shear loading. Plate size, $h/c = 1$; crack length, $a/c = 2/3$; orientation angle, $\delta = 45^0$.

The effects of variation of the orientation angle δ and the a/c ratio are shown in table VIII and figures 16 and 17. There is an important observation which concerns the effects of the variation of the orientation angle in the shear problem. As far as δ-dependence is concerned, the orthotropic plate behaves differently in tension and in shear. In the tension problem it was found that the maximum H_1 values always occurred at $\delta = 90^0$ (specially orthotropic material), while in the shear problem it is obvious that the maximum H_2 is δ-dependent. However, in both the tension and shear problems the minimum values of the significant stress intensity factors occurred at $\delta = 0^0$, which designates the other type of special orthotropy.

As an illustration of the typical stress distribution on the line $y = 0$, $1 < x/a \leq 3/2$, the values of the stress components were recorded in table IX and depicted in figures 18 and 19 for a plate with $a/c = 2/3$ and $\delta = 45^0$. Both σ_{xx} and σ_{yy} were found to be zero on the line $y = 0$, $1 < x/a \leq 3/2$ with $E_{22}/E_{11} = 1$ and for any value of

$$\frac{\frac{E_{11}}{E_{22}}}{\left(\frac{E_{11}}{2G_{12}} - \nu_{12}\right)^2}$$

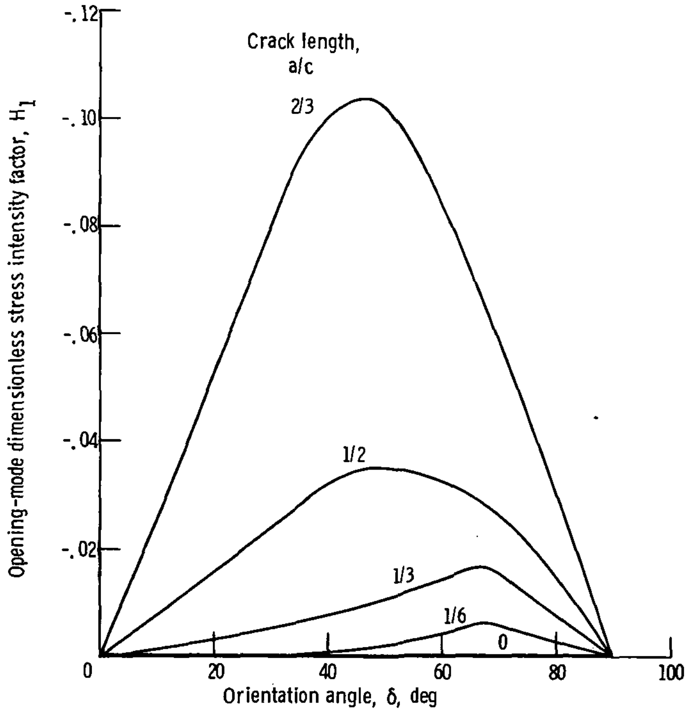

Figure 16. - Effects of orientation angle and plate width on opening-mode stress intensity factor for shear loading. Plate size, h/c = 1.

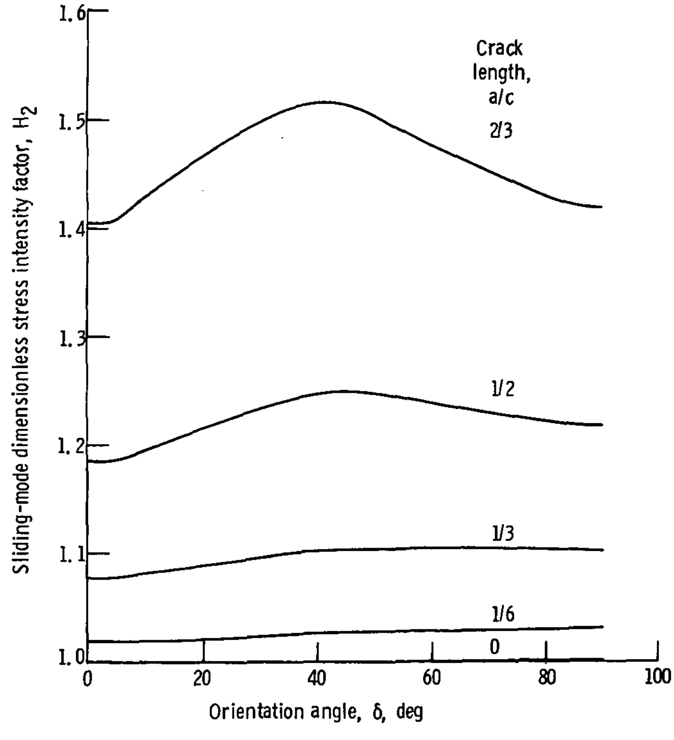

Figure 17. - Effects of orientation angle and plate width on sliding-mode stress intensity factor for shear loading. Plate size, h/c = 1.

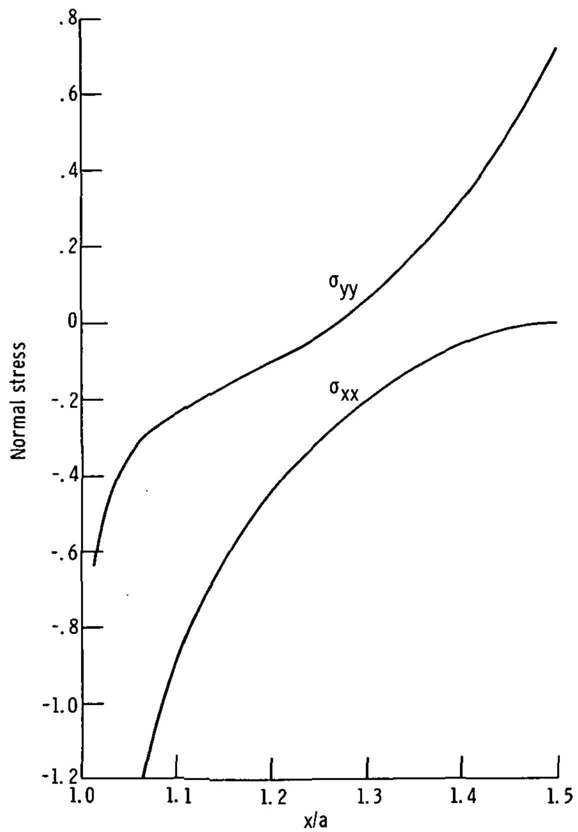

Figure 18. - Normal stress distribution on $y = 0$, $x > a$ line for shear loading. Plate size, $h/c = 1$; crack length, $a/c = 2/3$; orientation angle, $\delta = 45^0$; constant shear stress, $T_S = 1$.

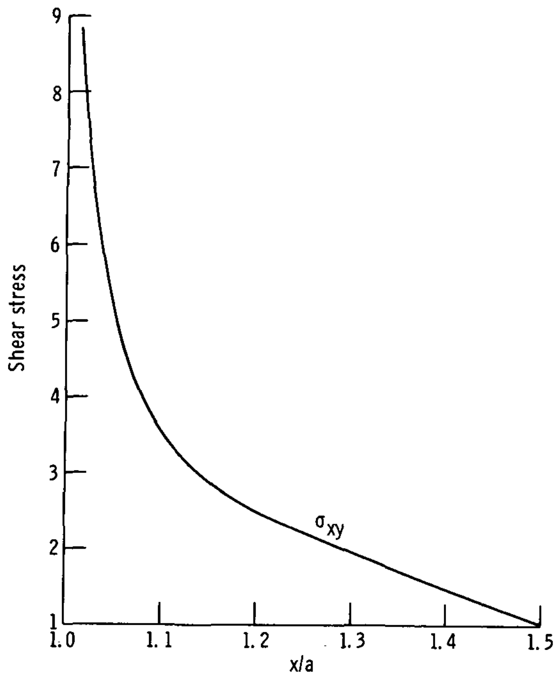

Figure 19. - Shear stress distribution on $y = 0$, $x > a$ line for shear loading. Plate size, $h/c = 1$; crack length, $a/c = 2/3$; orientation angle, $\delta = 45^0$; constant shear stress, $T_S = 1$.

The special cases of isotropy and special orthotropy resulted also in zero values for the normal stresses σ_{xx} and σ_{yy} on the $y = 0$, $1 < x/a \leq 3/2$ line.

CONCLUDING REMARKS

The mapping-collocation method as developed in reference 10 was applied to a large number of rectangular orthotropic plate problems in order to study the effects of varying material properties, orientation angles, and crack-length-to-plate-width a/c and plate-height-to-plate-width h/c ratios on the stress intensity factors for both tensile and shear loadings.

A natural extension of the mapping-collocation method as applied to finite orthotropic regions with centrally located traction-free cracks would be to consider various shapes for the inner boundary. For example, triangular, rectangular, and elliptical boundaries could be specified by a single general Schwarz-Christoffel transformation and mapped into the unit circle. This possibility would require further research as to the accuracy of the method when it is applied to various types of doubly connected regions.

Another direction of research presents itself in the consideration of a more detailed parametric study of the effects of dimensionless material constants, orientation angles, a/c ratios, and h/c ratios on the stress intensity factors. It is a possibility that, for certain parameter ranges, "practical forms" of expressions could be obtained for the approximation of the stress intensity factors. These forms would result from curve fitting the various parametric data.

Lewis Research Center,
National Aeronautics and Space Administration,
Cleveland, Ohio, September 21, 1972,
501-22.

REFERENCES

1. Lekhnit͡skiĭ, S. G. (P. Fern, trans.): Theory of Elasticity of an Anisotropic Elastic Body. Holden-Day, Inc., 1963.
2. Lekhnit͡skiĭ, S. G. (Elbridge Z. Stowell, trans.): Anisotropic Plates. American Iron and Steel Institute, 1956.
3. Savin, G. N. (Eugene Gros, trans.): Stress Concentration Around Holes. Pergamon Press, 1961.

4. Savin, G. N.: Stress Distribution Around Holes. NASA TT F-607, 1970.

5. Green, A. E.; and Zerna, W.: Theoretical Elasticity. Second ed., Oxford University Press, 1968.

6. Milne-Thomson, L. M.: Plane Elastic Systems. Second ed., Springer-Verlag, 1968.

7. Ang, D. D.; and Williams, M. L.: Combined Stresses in an Orthotropic Plate Having a Finite Crack. J. Appl. Mech., vol. 28, no. 3, Sept. 1961, pp. 372-378.

8. Mendelson, Alexander; and Spero, Samuel W.: Elastic Stress Distribution in a Finite-Width Orthotropic Plate Containing a Crack. NASA TN D-2260, 1964.

9. Gandhi, Kanu R.: Analysis of an Inclined Crack Centrally Placed in an Orthotropic Rectangular Plate. Rep. AMMRC-TR-71-31, Army Materials and Mechanics Research Center (AD-730911), Aug. 1971.

10. Gyekenyesi, George S.: Elastostatic Stress Analysis of Finite Anisotropic Plates with Centrally Located Traction-Free Cracks. Ph.D. Thesis, Michigan State University, 1972.

11. Bowie, O. L.; and Freese, C. E.: Central Crack in Plane Orthotropic Rectangular Sheet. Int. J. Fracture Mech., vol. 8, no. 1, Mar. 1972, pp. 49-58.

12. Bowie, Oscar L.; and Neal, Donald M.: A Modified Mapping-Collocation Technique for Accurate Calculation of Stress Intensity Factors. Rep. AMMRC-TR-69-28, Army Materials and Mechanics Research Center (AD-702248), Nov. 1969.

13. Muskhelishvili, N. I. (J. R. M. Radok, trans.): Some Basic Problems of the Mathematical Theory of Elasticity. P. Noordhoff, Ltd., 1953.

14. Altmann, S. L.: The Cellular Method for a Close-Packed Hexagonal Lattice. II. The Computations: A Program for a Digital Computer and an Application to Zirconium Metal. Proc. Roy. Soc. (London), Ser. A, vol. 244, no. 1237, Mar. 11, 1958, pp. 153-165.

15. Hulbert, Lewis E.: The Numerical Solution of Two-Dimensional Problems of the Theory of Elasticity. Ph.D. Thesis, Ohio State University, 1963.

16. Kobayashi, A. S.; Cherepy, R. D.; and Kinsel, W. C.: A Numerical Procedure for Estimating the Stress Intensity Factor of a Crack in a Finite Plate. J. Basic Eng., vol. 86, no. 4, Dec. 1964, pp. 681-684.

17. Isida, M.; and Itagoki, Y.: Stress Concentration at the Tip of a Central Transverse Crack in a Stiffened Plate Subjected to Tension. Proceedings of the Fourth U.S. National Congress of Applied Mechanics. Vol. 2, ASME, 1962.

18. Sawyer, Stephen G.: A Stress Intensity Factor Approach to the Analysis of Interfacial Cracks in Fiber Reinforced Composite Materials. Ph.D. Thesis, Carnegie-Mellon University, 1969.

TABLE I. - COMPARISON OF OPENING-MODE STRESS INTENSITY FACTORS FOR RECTANGULAR ISOTROPIC PLATES WITH CENTRAL CRACKS

[Plate size, h/c = 2.]

Crack length, a/c	Opening-mode nondimensional stress intensity factor, H_1			
	Kobayashi (ref. 16)	Isida (ref. 17)	Sawyer (ref. 18)	Present study
1/12	1.0048	1.0040	1.0094	1.0042
1/6	1.0191	1.0154	1.0253	1.0171
1/4	1.0448	1.0392	1.0509	1.0395
1/3	1.0830	1.0750	1.0737	1.0733
1/2	1.2215	1.1725	1.1443	1.1877
2/3	1.4665	1.4142	1.3804	1.4162

TABLE II. - TYPICAL PATTERN OF CONVERGENCE OF STRESS INTENSITY FACTORS FOR TENSILE LOADING

[Plate size, h/c = 1; crack length, a/c = 1/2; orientation angle, δ = 45°.]

Number of equations	Number of unknowns							
	15		25		41		83	
	H_1	H_2	H_1	H_2	H_1	H_2	H_1	H_2
16	1.3548	-0.0377	------	-------	------	-------	------	-------
24	1.3466	-.0394	------	-------	------	-------	------	-------
32	1.3455	-.0397	------	-------	------	-------	------	-------
40	------	-------	1.3531	-0.0461	------	-------	------	-------
48	------	-------	------	-------	1.3567	-0.0475	------	-------
64	1.3451	-.0400	1.3520	-.0460	------	-------	------	-------
96	------	-------	------	-------	1.3562	-.0472	------	-------
128	1.3451	-.0402	1.3520	-.0461	1.3562	-.0472	------	-------
176	------	-------	------	-------	------	-------	1.3563	-0.0472

TABLE III. - EFFECTS OF MATERIAL PROPERTIES ON STRESS INTENSITY FACTORS FOR TENSILE LOADING

[Plate size, h/c = 1; crack length, a/c = 2/3; orientation angle, δ = 45°.]

E_{11}/E_{22}	E_{22}/E_{11}											
$\left(\frac{E_{11}}{2G_{12}} - \nu_{12}\right)^2$	0.05		0.2		0.4		0.6		0.8		1.0	
	H_1	H_2	H_1	H_2	H_1	H_2	H_1	H_2	H_1	H_2	H_1	H_2
0.001	2.475	-0.651	2.358	-0.345	2.339	-0.189	2.320	-0.102	2.318	-0.006	2.392	-0.032
.050	2.006	-.387	1.805	-.184	1.741	-.099	1.735	-.057	1.731	-.024	1.730	0
.250	1.963	-.331	1.726	-.153	1.663	-.084	1.644	-.045	1.636	-.020	1.634	
.500	1.964	-.318	1.712	-.144	1.646	-.078	1.624	-.042	1.617	-.018	1.614	
.750	1.967	-.311	1.709	-.140	1.639	-.076	1.618	-.041	1.610	-.017	1.607	
1.000	1.972	-.307	1.707	-.139	1.636	-.075	1.614	-.041	1.605		1.604	
2.000	1.983	-.300	1.706	-.134	1.634	-.072	1.610	-.040	1.601		1.600	
4.000	1.994	-.296	1.710	-.131	1.635	-.071	1.610	-.040	1.601		1.602	
10.000	2.008	-.291	1.714	-.129	1.638	-.069	1.614	-.038	1.604		1.603	
100.000	2.034	-.287	1.727	-.127	1.648	-.069	1.622	-.038	1.612		1.611	
∞	2.048	-.284	1.735	-.127	1.655	-.069	1.629	-.038	1.619		1.618	

TABLE IV. - EFFECTS OF CRACK LENGTH AND PLATE SIZE ON STRESS INTENSITY FACTORS FOR TENSILE LOADING

[Orientation angle, δ = 45°.]

Crack length, a/c	Plate size, h/c											
	1/4		1/2		1		2		4		133	
	H_1	H_2	H_1	H_2	H_1	H_2	H_1	H_2	H_1	H_2	H_1	H_2
0	1.000	0.000	1.000	0.000	1.000	0.000	1.000	0.000	1.000	0.000	1.000	0
1/6	1.417	-.055	1.117	-.016	1.040	-.006	1.023	-.006	1.023	-.006	1.006	
1/3	2.331	-.199	1.450	-.062	1.157	-.021	1.093	-.021	1.089	-.021	1.017	
1/2	3.465	-.400	2.020	-.151	1.356	-.047	1.232	-.045	1.214	-.045	1.038	
2/3	4.946	-.680	2.999	-.288	1.669	-.091	1.497	-.082	1.460	-.076	1.069	

TABLE V. - EFFECTS OF CRACK LENGTH AND ORIENTATION ANGLE

ON STRESS INTENSITY FACTORS FOR TENSILE LOADING

[Plate size, h/c = 1.]

Orientation angle, δ, deg	Crack length, a/c									
	0		1/6		1/3		1/2		2/3	
	H_1	H_2	H_1	H_2	H_1	H_2	H_1	H_2	H_1	H_2
0	1.000	0	1.028	0	1.107	0	1.239	0	1.457	0
2			1.028	0	1.107	0	1.239	-.003	1.457	-.006
5			1.028	0	1.109	-.001	1.242	-.006	1.460	-.014
20			1.030	-.001	1.117	-.007	1.265	-.023	1.509	-.054
36			-----	-----	-----	-----	-----	-----	1.605	-.082
40			-----	-----	-----	-----	-----	-----	1.634	-.088
45			1.040	-.006	1.150	-.021	1.356	-.467	1.669	-.091
50			-----	-----	-----	-----	-----	-----	1.704	-.092
52			-----	-----	1.177	-.026	1.393	-.052	-----	-----
56			1.048	-.007	1.189	-.027	1.416	-.054	1.745	-.091
60			1.052	-.008	1.202	-.028	1.438	-.055	-----	-----
62			-----	-----	-----	-----	1.450	-.055	-----	-----
64			1.057	-.009	1.215	-.030	1.460	-.054	-----	-----
68			1.059	-.008	1.226	-.028	-----	-----	-----	-----
70			1.061	-.007	1.232	-.027	1.489	-.048	1.829	-.068
85			1.069	-.003	1.256	-.009	1.532	-.014	1.881	-.018
88			1.071	-.001	1.259	-.003	1.535	-.006	1.884	-.008
90			1.071	0	1.259	0	1.535	0	1.884	0

TABLE VI. - STRESS DISTRIBUTION ON y = 0, x > a

LINE FOR TENSILE LOADING

[Plate size, h/c = 1; crack length, a/c = 2/3; orientation angle, $\delta = 45^{\circ}$; constant tensile stress, $T_t = 1$.]

x/a	Components of stress tensor (rectangular coordinates)		
	σ_{xx}	σ_{yy}	σ_{xy}
1.016	7.33	9.59	-0.482
1.046	3.54	5.53	-.227
1.076	2.37	4.27	-.131
1.106	1.74	3.58	-.069
1.136	1.33	3.12	-.021
1.166	1.04	2.77	.020
1.196	.81	2.50	.055
1.228	.63	2.26	.085
1.258	.49	2.05	.111
1.288	.37	1.86	.131
1.318	.26	1.67	.146
1.348	.18	1.50	.153
1.374	.11	1.33	.150
1.410	.06	1.17	.136
1.440	.03	1.01	.108
1.470	0	.84	.063
1.500	0	.68	0

TABLE VII. - EFFECTS OF MATERIAL PROPERTIES ON STRESS INTENSITY

FACTORS FOR SHEAR LOADING

[Plate size, h/c = 1; crack length, a/c = 2/3; orientation angle, $\delta = 45^{\circ}$]

$\dfrac{E_{11}/E_{22}}{\left(\dfrac{E_{11}}{2G_{12}} - \nu_{12}\right)^2}$	E_{22}/E_{11}											
	0.05		0.2		0.4		0.6		0.8		1.0	
	H_1	H_2	H_1	H_2	H_1	H_2	H_1	H_2	H_1	H_2	H_1	H_2
0.001	-0.629	2.231	-0.330	2.113	-0.189	2.078	-0.103	2.068	-0.042	2.062	-0.017	2.075
.050	-.424	1.799	-.216	1.644	-.117	1.591	-.067	1.588	-.030	1.584	0	1.583
.250	-.345	1.720	-.170	1.555	-.093	1.512	-.052	1.498	-.023	1.494		1.492
.500	-.315	1.700	-.151	1.530	-.084	1.487	-.047	1.472	-.020	1.467		1.464
.750	-.301	1.692	-.143	1.519	-.078	1.474	-.042	1.460	-.018	1.454		1.453
1.000	-.291	1.687	-.136	1.512	-.075	1.467	-.040	1.451	-.018	1.447		1.446
2.000	-.270	1.679	-.123	1.498	-.067	1.451	-.037	1.437	-.017	1.431		1.430
100.000	-.215	1.670	-.088	1.468	-.047	1.419	-.027	1.402	-.011	1.396		1.395
∞	-.209	1.669	-.081	1.464	-.042	1.413	-.023	1.396	-.010	1.390		1.389

TABLE VIII. - EFFECTS OF PLATE WIDTH AND ORIENTATION ANGLE ON STRESS INTENSITY FACTORS FOR SHEAR LOADING

[Plate size, h/c = 1.]

Orientation angle, δ, deg	Crack length, a/c									
	0		1/6		1/3		1/2		2/3	
	H_1	H_2	H_1	H_2	H_1	H_2	H_1	H_2	H_1	H_2
0	0	1.000	0	1.018	0	1.075	0	1.187	0	1.406
2			-----	1.018	0	1.075	0	1.187	-.004	1.406
5			-----	1.018	0	1.076	-.003	1.189	-.011	1.410
20			-----	1.021	-.003	1.089	-.016	1.218	-.052	1.467
34			-----	-----	-----	-----	-----	-----	-.091	1.511
38			-----	-----	-.007	1.102	-.031	1.246	-.098	1.516
42			-----	-----	-----	-----	-----	-----	-.102	1.516
44			-----	-----	-.010	1.105	-.034	1.249	-.103	1.516
45			-.001	1.025	-.010	1.105	-.034	1.249	-.103	1.515
46			-----	-----	-----	-----	-----	-----	-.103	1.513
48			-----	-----	-----	-----	-.035	1.247	-----	-----
50			-----	-----	-.011	1.105	-.035	1.247	-.102	1.508
54			-----	-----	-.013	1.106	-.034	1.243	-----	-----
58			-----	-----	-.014	-----	-----	-----	-----	-----
62			-----	-----	-.016	-----	-----	-----	-----	-----
64			-.006	1.028	-----	-----	-----	-----	-----	-----
66			-----	-----	-.017	-----	-----	-----	-----	-----
68			-----	-----	-.017	1.105	-----	-----	-----	-----
70			-.006	1.028	-.016	1.105	-.027	1.229	-.058	1.453
85			-.001	-----	-.006	1.102	-.009	1.218	-.014	1.421
88			0	-----	-.003	1.102	-.003	1.218	-.006	1.421
90			0	-----	0	1.102	0	1.218	0	1.421

TABLE IX. - STRESS DISTRIBUTION ON $y = 0$, $x > a$

LINE FOR SHEAR LOADING

[Plate size, $h/c = 1$; crack length, $a/c = 2/3$; orientation angle, $\delta = 45^{\circ}$; constant shear stress, $T_s = 1$.]

x/a	Components of stress tensor (rectangular coordinates)		
	σ_{xx}	σ_{yy}	σ_{xy}
1.016	-3.01	-0.60	8.77
1.046	-1.55	-.36	5.14
1.076	-1.09	-.28	4.02
1.106	-.085	-.23	3.43
1.136	-.68	-.19	3.04
1.166	-.56	-.15	2.76
1.196	-.46	-.11	2.53
1.228	-.37	-.07	2.34
1.258	-.29	-.03	2.17
1.288	-.23	.03	2.01
1.318	-.18	.09	1.87
1.348	-.12	.17	1.72
1.374	-.08	.25	1.58
1.410	-.04	.35	1.44
1.440	-.02	.46	1.30
1.470	0	.58	1.15
1.500	0	.72	1.00

NASA-Langley, 1972 —— 32 E-6889

"The aeronautical and space activities of the United States shall be conducted so as to contribute . . . to the expansion of human knowledge of phenomena in the atmosphere and space. The Administration shall provide for the widest practicable and appropriate dissemination of information concerning its activities and the results thereof."

—NATIONAL AERONAUTICS AND SPACE ACT OF 1958

NASA SCIENTIFIC AND TECHNICAL PUBLICATIONS

TECHNICAL REPORTS: Scientific and technical information considered important, complete, and a lasting contribution to existing knowledge.

TECHNICAL NOTES: Information less broad in scope but nevertheless of importance as a contribution to existing knowledge.

TECHNICAL MEMORANDUMS: Information receiving limited distribution because of preliminary data, security classification, or other reasons. Also includes conference proceedings with either limited or unlimited distribution.

CONTRACTOR REPORTS: Scientific and technical information generated under a NASA contract or grant and considered an important contribution to existing knowledge.

TECHNICAL TRANSLATIONS: Information published in a foreign language considered to merit NASA distribution in English.

SPECIAL PUBLICATIONS: Information derived from or of value to NASA activities. Publications include final reports of major projects, monographs, data compilations, handbooks, sourcebooks, and special bibliographies.

TECHNOLOGY UTILIZATION PUBLICATIONS: Information on technology used by NASA that may be of particular interest in commercial and other non-aerospace applications. Publications include Tech Briefs, Technology Utilization Reports and Technology Surveys.

Details on the availability of these publications may be obtained from:

SCIENTIFIC AND TECHNICAL INFORMATION OFFICE

NATIONAL AERONAUTICS AND SPACE ADMINISTRATION

Washington, D.C. 20546